

Desing spectrums for the central north of quito and seismic analysis of steel structures using the capacity spectrum method

Roberto Aguiar¹, David Mora², Enrique Morales³, Santiago Trujillo⁴, Michael Rodriguez⁴

ABSTRACT

The city of Quito lies on geological faults that have no surface outcrop but are moving with a speed of 2-4 mm per year. The last strong earthquake associated with these thrust faults, was recorded in 1587 and had a magnitude of 6.4; so it has been more than 400 years, there is a large amount of stored energy, and the probability of an earthquake occurring is very high. Therefore, this article presents, firstly, the periods of recurrence of these faults; then a microzoning of the north central part of the city and the elastic response spectra for 5% damped associated to the Llumbisi- La Bota segment fault, ILB. And subsequently, an analysis of nine steel structures from one to nine storeys assuming that they are situated in the following three areas of north central Quito: the old Quito Tenis; La Gasca and Benalcazar High School. Using the Capacity Spectrum Method MEC, the seismic response is found with the presence of three spectrums as prescribed in the Ecuadorian Construction Regulations NEC-11; the recommendation in the study of the seismic microzoning of Quito ERN-12 and those found in the seismic microzoning associated with the fault ILB. Three types of responses are indicated for each location, the structures situated in the old Quito Tenis present a performance point found using the Capacity Spectrum Method MEC; for those in La Gasca, a maximum lateral displacement is indicated in each storey; and the structures situated in the Benalcazar High School present maximum interstorey drifts. It should be highlighted that the lateral displacements and interstorey drifts are reaching the end of their performance, thus the conclusions to be found in this study about which spectrum the maximum response has could be inferred from any of the three structural parameters.

Keywords: Design spectrums, Quito, Seismic Analysis, and Capacity Design Method.

http://dx.doi.org/17196/rsee.v12i3/5222

Department of Earth Sciences and Construction. University of the Ecuadorian Army – ESPE: Av. Gral. Rumiñahui s/n, Valle de los Chillos, Quito, Ecuador, E-mail: rraguiar@espe.edu.ec.

² Faculty of Civil and Environmental Engineering. National Polytechnic School EPN: Av Ladron de Guevera E11-253, Quito, Ecuador.

³ Graduate Research Assistant - Department of Civil, Structural and Environmental Engineering, State University of New York at Buffalo, Buffalo, NY, 14260, U.S.A., E-mail: enriquea@buffalo.edu.

Graduate Research Assistant -Department of Earth Sciences and Construction. University of the Ecuadorian Army – ESPE: Av. Gral. Rumiñahui s/n, Valle de los Chillos, Quito, Ecuador.

1 Introduction

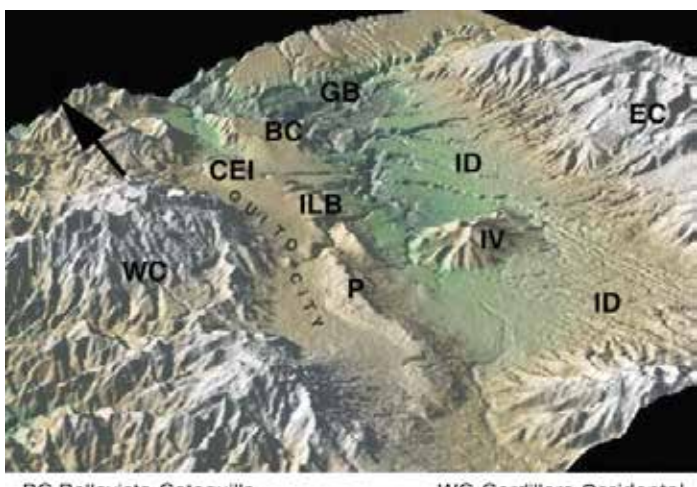
The constant movement of the Nazca plate situated opposite the American plate, in Ecuador, has given rise to the Carnegie ridge located in the Pacific Ocean, to the subduction trench, and to the mega faults which begin in the Gulf of Guayaquil, pass through Colombia by the Romeral faults and end in Venezuela, in the Boconó faults.

Forming part of this mega fault is a system of blind inverse faults spanning the city of Quito, which can be seen in figure 1, and from south to north are the inverse faults of: Puengasí (P), Llumbisí-La Bota (ILB), Carcelén-El Inca (CEI) and Bella Vista-Catequilla (BC).

Figure 2 shows a numerical calculation model of possible fault planes that could be generated in the case of earthquakes occuring with a burst length equal to the maximum distance of each of the fault segments. The model assumes that these events are not produced simultaneously (Alvarado et al. 2014; Rivas et al. 2014). The fault planes are shown projected in a horizontal plane.

The largest recorded earthquake associated with the blind faults is that of 1587 which had a magnitude of 6.4, with a shallow focal point (Beuval et al. 2010). This is very worrying as much of the city lies on the same faults (on the slopes of the mountains) and hopefully their foundations are well anchored to the ground, because the vertical component will be very high, as happened in the earthquake of Christchurch, New Zealand (2011), to cite one of the most recent associated with blind faults under a city.

Figure 1: Quito bounded on the west by the western mountains and east by the fault system: Puengasí (P), Ilumbisí-La Bota (ILB) and crossed by the Inca Carcelén (CEI). (Alvarado et al. 2014).



BC Bellavista-Catequilla ID Depresión Interandina IV volcan IIaló

GB Cuenca Guayllabamba

WC Cordillera Occidental EC Cordillera Oriental P Puengasí ILB Ilumbisí-La Bota

CEI Carcelén-El Inca

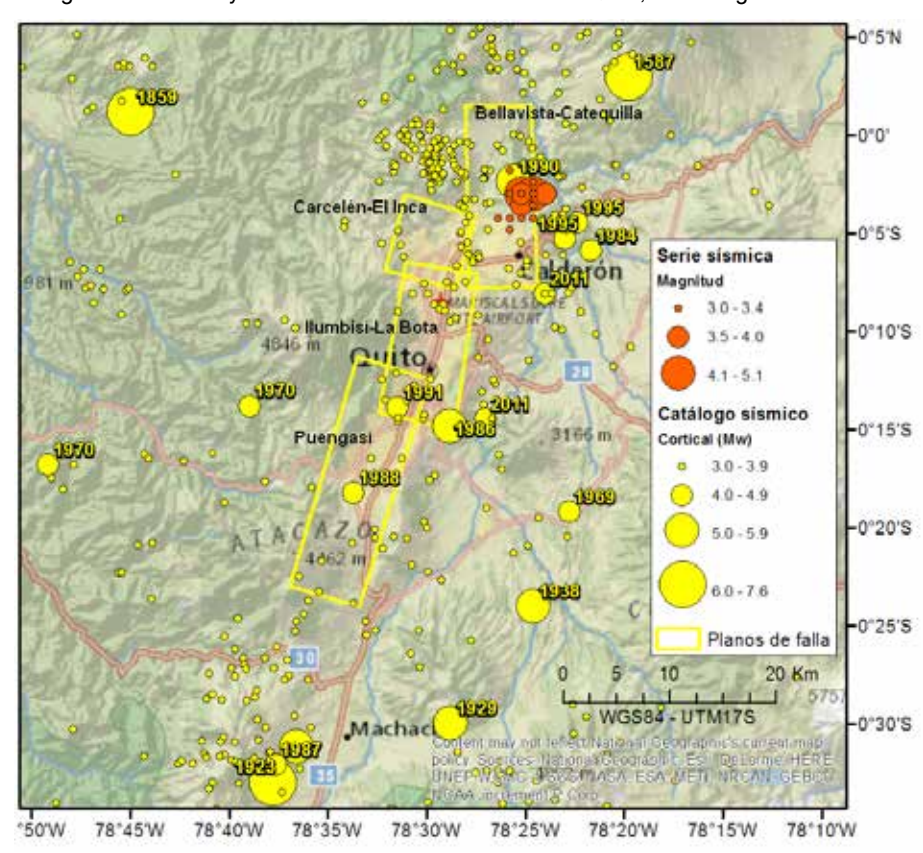


Figure 2: Seismicity associated with the blind faults of Quito, excluding that of 1859.

The Christchurch earthquake of 2011, had a magnitude of 6.2, a deep focal point of 5 km, was associated with an oblique inverse fault with an inclination 700 and the city floor had shear wave speeds that were around 300 m/s2. The maximum recorded acceleration in the zone of the epicenter was $2.2\,g$ nearly double the maximum horizontal acceleration. (Elwood, 2013; Kam and Pampanin, 2011). This earthquake may give us light as to how to be more careful in the design of structures situated around of the blind inverse faults.

Table 1 indicates the periods of recurrence found for each one of the sectors of Quito's blind faults, found for different magnitude ranges, using the modified model of Gutenberg and Richter, it can be seen that for earthquakes of the highest magnitude or equal to 6 and less than the maximum expected magnitude ([6,0]) the periods of recurrence are found between 164 and 290 years. (Rivas et al. 2014)

Table 1: Period of recurrence, found using the modified model of Gutenberg and Richter.

Range of magnitude	Period of recurrence (years)									
	PUESGASÍ	ILB	CEI	вс	Tangahuilla					
[5,0 - 5,5)	20 - 35	18 - 30	27 - 39	18 - 31	23 - 34					
[5,5 - 6.0)	62 - 87	56 - 75	85 - 130	58 - 78	65 - 97					
[6,0 <	164 - 262	179 - 279		169 - 279	179 - 290					
Mmax	1224 - 2190 (Mw6,4)	610 - 981 (Mw6,2)	549 - 952 (Mw5,9)	908 - 1630 (Mw6,3)	579 - 1016 <i>(Mw6,0)</i>					

The last row of Table 1, shows the maximum expected magnitude in each segment, found by applying the equations of Leonard (2010) and the period of recurrence is expressed as a time interval; the lower intervals are given in the earthquakes of lower magnitude and the one which has the highest floating population density is Ilumbisí-La Bota with around 500 habitants per hectare, for this reason a seismic microzoning study was carried out for north central Quito since many of their constructions are situated in this fault segment.

2 Microzoning of North Central Quito

On the left of figure 3 are the north central boroughs and a calculation grid. At each point three spectra associated with an earthquake of magnitude 6.2 were found, which are thought to be located directly in the center of gravity of the fault Ilumbisi-La Bota (ILB); the fault plane can be seen on the right of the figure, with slanted stripes. The spectra were found to match the models of strong movement of Campbell and Borzognia (2013), Abrahamson, Silva and Kamai (2013) and Zhao et al. (2006), in short form identified as A & B, A,S & K, and Zhao.

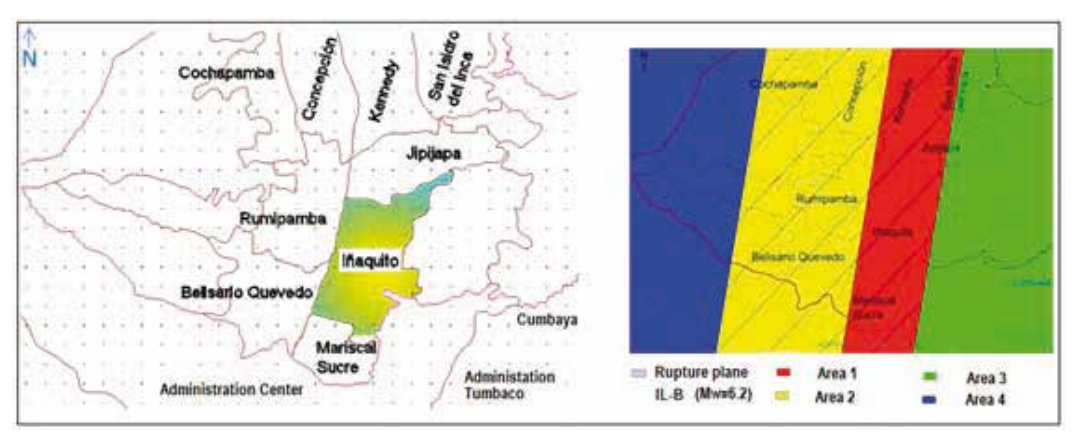


Figure 3: Grid of study and microzoning of North Central Quito

The study conducted (Trujillo 2014, Aguiar et al. 2015) obtained four micro zones which are indicated at the right of figure 4. Zone 1 is the most dangerous because it is in the hanging wall and is on the ILB segment. The least dangerous is that found outside the fault plane.

Elastic response spectra were found for a level of reliance of 84% and were obtained by weighing up the following: 35% of the model of C & B; 35% of the model of A, S & K and 30% of the model of Zhao. The spectra found are shown in figure 4.

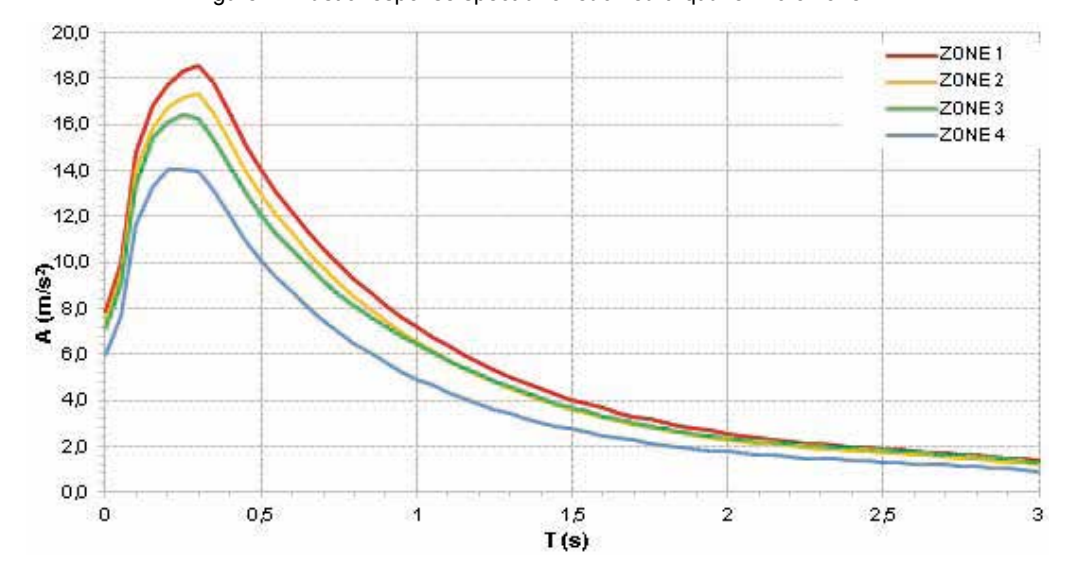


Figure 4: Elastic response spectra for each earthquake micro zone.

3 NEC-11 And ERN-12 Response Spectrums

For the area of short periods, less than 0.5 seconds, the ordinates of the spectra associated with the ILB fault are higher than those reported by The Ecuadorian Construction Regulations (Norma Ecuatoriana de la Construcción, NEC-11), or those that are obtained based on site factors found in the earthquake microzoning study of ERN-12 (Aguiar 2013). However, for intermediate periods and larger, they are less than those found with the NEC-11 or ERN-12.

Figure 5: Shear wave velocities in three areas of North Central Quito.

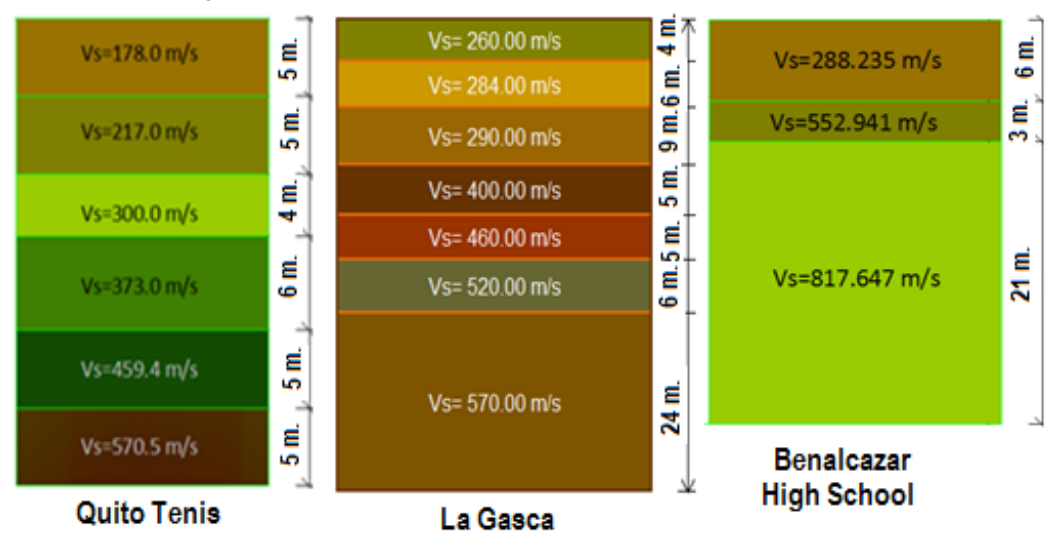


Figure 5 shows the shear wave velocity $V_{\rm S}$ in three sectors of north central Quito, which are the old Quito Tenis, which is located in zone 2; La Gasca which can be found in zone 1 and Benalcazar High School which is situated in zone 2, of the microzoning. For these three sites it is subsequently considered that they all have steel structures from one to nine storeys.

The site factors of the NEC-11 are at the macro level, valid and applicable to all of Ecuador. However, those of ERN-12 correspond to the land type of the city of Quito but were calibrated to use the same equations of NEC-11. With this in mind, table 2 presents the site factors for the three sites of figure 5; furthermore, indicating in which zone they are in accordance with figure 3.

Table 2: Site factors for the sites of North Central Quito following NEC-11 and ERN-12

Site	"Quito Tenis"			"La Gasca"			"Benalcazar" High school		
Factors	NEC11	ERN12	ILB	NEC11	ERN12	ILB	NEC11	ERN12	ILB
Fa	1.20	1.155		1.20	1.055		1.20	1.255	
Fd	1.40	0.575	Zone2	1.40	1.505	Zone1	1.30	1.105	Zone2
Fs	1.50	1.790		1.50	0.740		1.30	1.225	

The spectra obtained with the data in table 2 is shown in figure 6, where it is clear that, for all cases, in the area of short periods, the spectral ordinates that are generated from the earthquake of 6.2 magnitude in fault ILB is considerably higher than those found with NEC-11 or ERN-12; this may lead one to think that it is safer to calculate

all of the structures located in north central Quito with the spectrum of ILB, which is actually false, as you will see later.

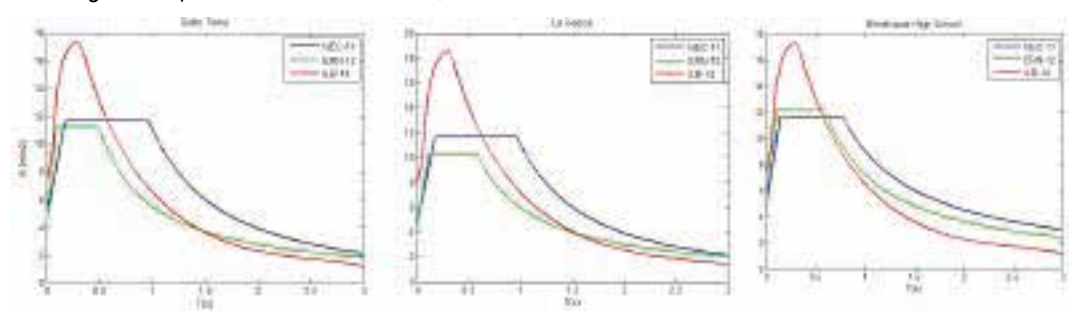


Figure 6: Spectra found with NEC-11, ERN-12 and ILB for three sectors of north central Quito.

4 Seismic analysis of steel structures.

It was deemed that all of the frames of the steel structures of 1 to 9 storeys have three bays each, with 7.315 m. lights, and mezzanine heights of 3.81 m., equal in all the storeys; the uniform load in each storey is 3.269 T/m. Also indicated are the sections of the "I" steel profiles; it is clear that the exterior columns have a larger transversal section than the interior columns.

..... 3.269 T/m 3.269 T/m 4 @ 3.810 m = 15.240 W27X94 3.269 T/m 3.269 T/m 2 @ 3.810 m = 7.620 W30X99 W30X99 W30X99 W30X99 W30X99 W30X99 14X193 3.269 T/m 3.269 T/m W30X99 3 @ 7.315 m = 21.945 3 @ 7.315 m = 21.945

Figure 7: Geometry and loads of the buildings of a 4 storey and a 2 storey.

Figure 7 serves to explain the sections used, for all of the structures analysed and presented in table 3. The 2 storey structure has columns with W14X193 profiles in the exterior part and W30X173; these sections remain in all of the analysed 1 to 9 storey structures. Therefore, they can be seen in the first two storeys of the four storey frame whilst in the third and fourth storeys W14X159 and W27X146 profiles are shown. For those of six storeys the structures remain the same for the first four storeys and for the fifth and sixth appear as W14X109 y W24X104 profiles. A similar pattern is followed for beams.

On the other hand, working with symmetrical sections and uniform sections, the moment curvature diagram, in the initial node, is equal to that of the center of light and the final node; furthermore, these values are equal if there is traction on the lower fibers or the upper fibers, in the case of beams; and it is a similar thing for columns. Therefore, in table 3 the yield moment indicated M_y and its associated curvature \varnothing_y and the moment formed by the plastic ball-and-socket M_u and its associated curvature \varnothing_u need no further explanation. In the case of columns, the third column indicates the movement of the axial load.

Table 3: Sections, the moment curvature diagram and axial stiffness of columns

Floors	Section	Р	M _y	M _u	Ø _v	\varnothing_{u}	EA
	Section	(T.)	(Tm.)	(Tm.)	(1/m)	(1/m)	(T.)
1 & 2	W14X193	927.12	147.18	176.62	0.00702	0.07718	769546.85
1 & 2	W30X173	832.45	251.66	301.99	0.00350	0.03848	690966.36
3 & 4	W14X159	762.26	118.99	142.79	0.00716	0.07881	632708.41
3 & 4	W27X146	703.50	192.37	230.85	0.00389	0.04277	583934.32
5 & 6	W14X109	522.32	79.60	95.52	0.00734	0.08079	433547.52
5 & 6	W24X104	499.47	119.82	143.78	0.00442	0.04864	414579.82
7 & 8	W14X99	474.99	71.72	86.07	0.00739	0.08132	394257.28
9	W14X82	391.74	57.63	69.15	0.00748	0.08232	325160.62

Table 4: Sections, the momentum curvature diagram and axial stiffness of beams

Floors	Section	M _y (Tm.)	M _u (Tm.)	Ø _y (1/m)	Ø _u (1/m)	EA (T.)
1 & 2	W30X99	129.35	155.22	0.00371	0.04080	394257.28
3 & 4	W27X94	115.26	138.31	0.00403	0.04436	375289.57
5 & 6	W24X76	82.92	99.50	0.00452	0.04969	303483.26
7 & 8	W24X62	63.43	76.12	0.00468	0.05150	246580.15
9	W21X48	44.36	53.23	0.00529	0.05821	191031.88

Figure 8: Bilinear model of the moment curvature diagram.

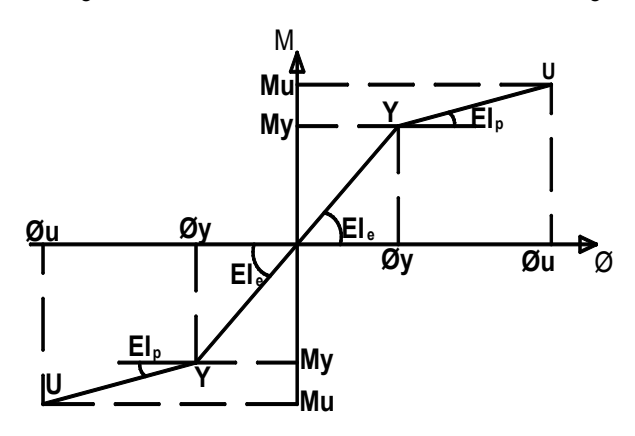


Figure 8 shows the bilinear model of the moment curvature diagram that was worked with. For the calculation of the elastic stiffness El_e it was deemed that a modulus of elasticity of steel was equal to $21000000T/m^2$. The yield moment was obtained with the following equation.

$$M_{v} = Z_{v} f y \tag{1}$$

Where Z_X is the plastic section modulus that is equal to the static moment of the areas of tension and compression in respect to its neutral axis $(Zx = \int y \ dA)$; fy is the yield stress of the steel, the steel used was ASTM A36 with.

With the elastic rigidity El_e ; and the yield moment $M_{_Y}$ the curvature of yield is determined $(\emptyset = M_Y/El_e)$. On the other hand, the rigidity in the inelastic range El_p has the following expression.

$$El_{\mathbf{p}} = \alpha \, El_{\mathbf{e}} \tag{2}$$

It is calculated with the value $\alpha=0.02$, which is a conservative value, much as $M_u=1.2~M_y$, which was the way that the plastic moment was obtained, is also considered a conservative value. Finally, the curvature \varnothing_v was obtained from the bilinear model shown in figure 8, with the following equation.

$$\phi_u = \frac{M_u - M_y + EI_p \,\phi_y}{EI_p} \tag{3}$$

All of the variables shown in equation (3) have been defined.

5 Capacity spectrum method

The resistant seismic capacity curve that relates to the base shear V with a lateral displacement at the top of the structure D_t is found, by means of non-lineal static analysis working with the concentrated plasticity model of Giberson (1969) and applying the lateral load increments in each storey, proportional to the first mode of vibration, employing the following equation. (ATC-40, 1996)

$$F_i = \frac{w_i \, \emptyset_i}{\sum w_i \, \emptyset_i} \, V_0 \tag{4}$$

Where the subindex i makes reference to the storey i; with this noted F is the lateral force; w the weight, \emptyset is the first mode of vibration and V_O is the base shear that is imposed on each one of the load cycles.

In Aguiar et al. (2015) the theoretical framework of resistant seismic capacity curves $V-D_t$ is well detailed, as well as the way that the capacity spectrum is obtained S_a-S_d , by means of the following equations:

$$S_{ai} = \frac{V_i}{\alpha_1 M_T} \tag{5}$$

$$S_{di} = \frac{D_{ti}}{FP_i} \tag{6}$$

Where D_{ti} V_i are the coordinates of a point on the resistant seismic capacity curve for which the displacement and spectral acceleration are determined S_{di} ; S_{ai} ; M_t is the total mass of the tructure; α_1 is the modal mass ratio of the first mode; FP_1 is the modal participation factor of the first mode.

$$\alpha_1 = \frac{(\phi_1^t M J)^2}{M_T (\phi_1^t M \phi_1)} \tag{7}$$

$$FP_i = \frac{\phi_1^t M J}{\phi_1^t M \phi_1} \tag{8}$$

The variables still not indicated are: M is the mass matrix; J is the vector of incidence of land movement with the lateral coordinates of the structure; in two dimensions J is a unitary vector. It is highlighted that the modal participation factor is obtained in

an absolute value. On the other hand, using the pseudo spectrum definition, the sought for spectra are found in the format S_d – S_a . Being S_a the spectral acceleration and S_d the spectral displacement. Finally, the Capacity Spectrum Method is applied which is very well detailed in Aguiar et al. (2015). However, it is indicated that the damping factor, for when the structure works in the non-linear range, is obtained employing a bilinear hysteresis model with the equation proposed by Jennings (1968)

$$\xi_{eq} = \frac{E_D}{4 \pi E_S} = \frac{2 (\mu - 1) (1 - \alpha)}{\pi \mu (1 + \alpha \mu - \alpha)}$$
(9)

Where E_D the energy is dissipated per cycle in hysteretic behavior; E_S is the strain energy stored elastically; α is the relationship between the post yield stiffness with respect to the elastic stiffness of the bilinear model; μ is the ductility demand.

The ATC-40 considering the imperfections of the hysteresis curves, in the sense that they are not straight as they were expected to be in the bilinear model without curves, introduces a correction factor K in accordance with the standard of the structural design. Such that the effective viscous absorption is:

$$\xi_{ef} = \xi + k \, \xi_{eq} \tag{10}$$

Where ξ is the inherent equivalent viscous damping of the structure. Once the damping factor is obtained ξ e f the respective inelastic spectrum is found by dividing the ordinates of the elastic spectrum by B.

$$B = \left(\frac{\xi_{ef}}{0.05}\right)^{0.3} \tag{11}$$

The interception of the capacity spectrum of the structure with the seismic demand spectrum determines the performance point, it should comply with the ductility demand by which the effective damping factor value is obtained and, subsequently, factor B is approximately equal to the ductility demand of the performance point, if not so, the calculation is repeated.

When the structure works in the elastic range, the interactive calculation is not made; in this case the performance point as well as the section point of the demand and capacity spectrum are obtained directly. But when the linear range is exceeded, the performance point is obtained interactively; in this case, in the graphs presented in the following section, the spectrum of initial seismic demand (elastic range) is shown and final with/ending whatever verifies the equality of ductilities, they are the graphs which are divided by *B*. Intermediate positions of calculation are not indicated.

6 Performance results point

Figure 8 shows 8 graphs; those in the first row correspond to the structures with 1 to 3 storeys; the second, to those with 4 to 6 storeys and the last three to those of 7 to 9 storeys. These graphs show the performance point of the structures situated in old Quito Tenis, i.e. using the spectrum found on the left in figure 6.

In figure 8 it is appreciated that the structures with 1 to 5 storeys work in the elastic range and, for these, the largest displacement of the point of demand is found with the spectrum associated with the fault Ilumbisi-La Bota (ILB). In contrast, for the structures with 6 to 9 storeys the largest displacements are found with the spectrum of the NEC-11.

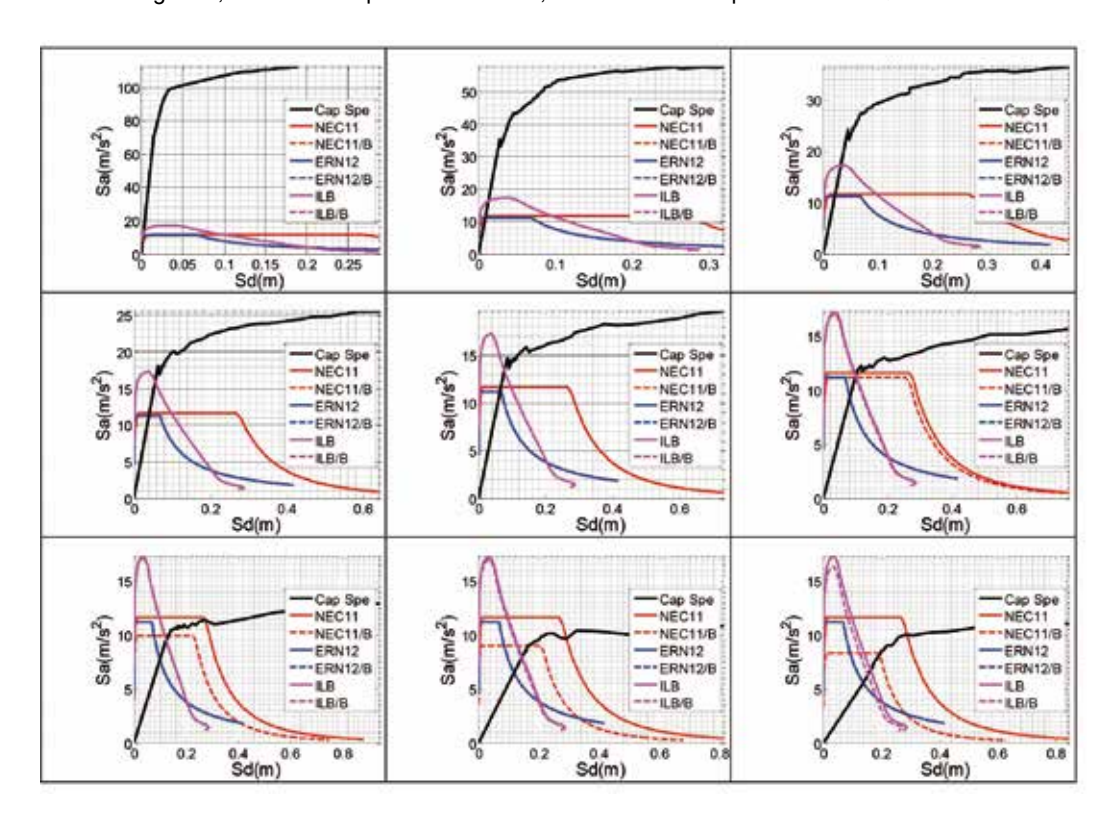


Figure 8; Performance point with NEC11, ERN12 and ILB Spectrums Old Quito Tenis.

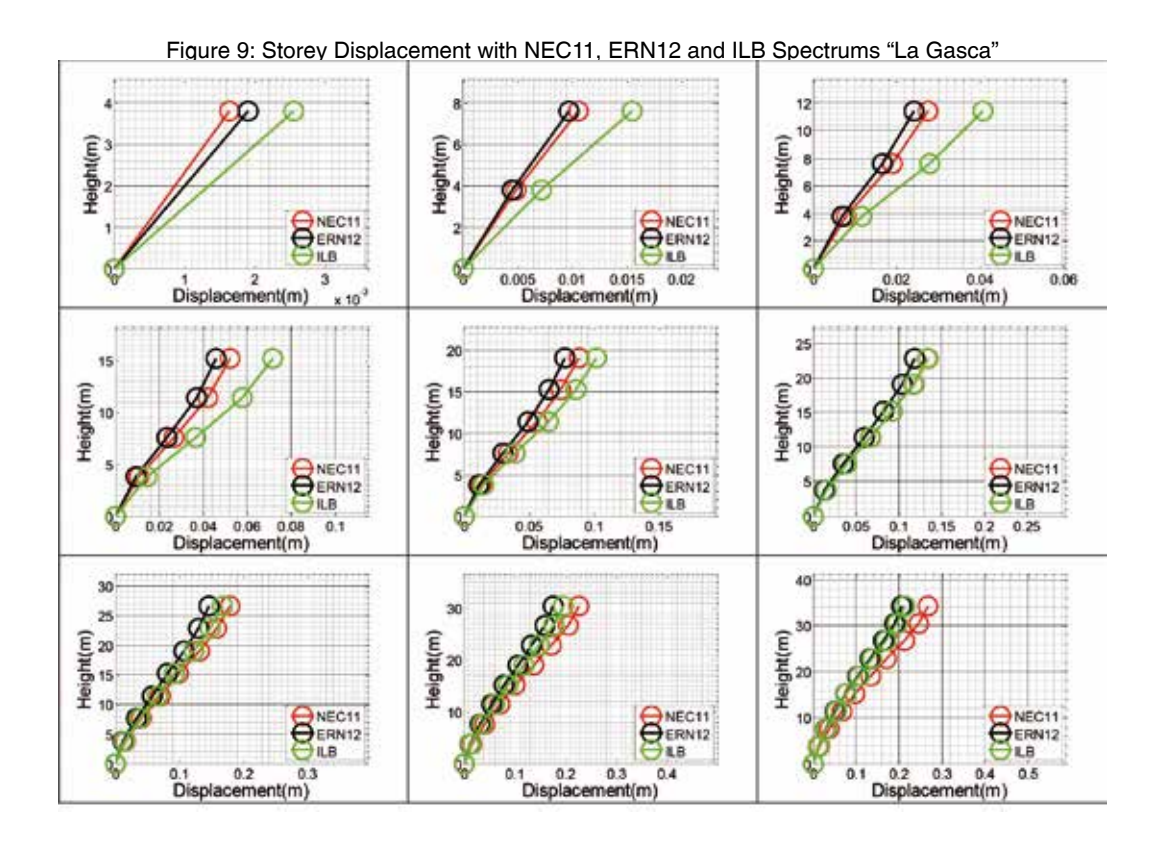
7 Storey displacement

Presented in the previous section, was the performance point of the structures with 1 to 9 storeys, situated in the old Quito Tenis; the structures situated at the other two sites have similar behavior. Therefore, a presentation of these is not included and in its place is a presentation of the lateral displacements in each storey that are obtained from the performance point considering that the structure works in the first mode of vibration.

It is noted that the displacement corresponding with the performance point S_d is not the maximum displacement of the structure, it is a displacement associated with a system of one degree of freedom, in order to position the displacement at the top D_y the equation (6) is used, i.e. S_d is multiplied by the factor of modal participation FP at the performance point. Finally, the displacements in each storey are found multiplying D_t by the first mode of vibration that was normalized to the unit at the top.

These results are shown for the structures situated in La Gasca, in the same format as figure 8, i.e. the graphs of the first row correspond to the lateral displacements of the structures with 1 to 3 storeys; in the second row come the lateral displacements of the structures with 4 to 6 storeys and the third row corresponds to the structures with 7 to 9 storeys.

In the structures with 1 to 6 storeys, the largest lateral displacements arise from the spectrum of Ilumbisí (ILB). For the structures with 7 to 9 storeys the maximum displacements are found applying the spectrum of the NEC-11. It is a result similar to that obtained in the previous section when working with the performance point.



8 Interstorey drifts

Another indicator of structural damage is the interstorey drift, figure 10 shows the interstorey drift found in the steel structures with 1 to 9 storeys, assuming that the buildings are located in the Benalcazar High school. For the structures with 1 to 5 storeys the largest values are found with the spectrum of Ilumbisi.

In the structures of 6 storeys the largest interstorey drifts are found with the spectrum ERN-12, this is the only case of those studied in which the largest seismic demands are found with this spectrum. In the structures with 7 to 9 storeys, the máximum interstorey drifts are found with the spectrum of the NEC-11.

Table 5 shows the fundamental periods of vibration of each one of the steel structures. Furthermore, as indicated, the structures with 1 to 5 storeys work in the elastic range, and those with 6 to 9 storeys had a small incursion in the inelastic range so that the vibration period in the performance point was practically the same as in the elastic range. The above is confirmed by the values of B (equation 11) seen/used with those that were obtained by the performance point of the structures situated in the old Quito Tenis. These values are shown in table 6

Table 5: Elastic periods in each steel structure

Floor	1	2	3	4	5	6	7	8	9
T(s)	0.09	0.18	0.27	0.37	0.48	0.59	0.72	0.86	1.01

Figure 10: Interstorey drift with NEC11, ERN12 and ILB Spectrums "Benalcazar" High school

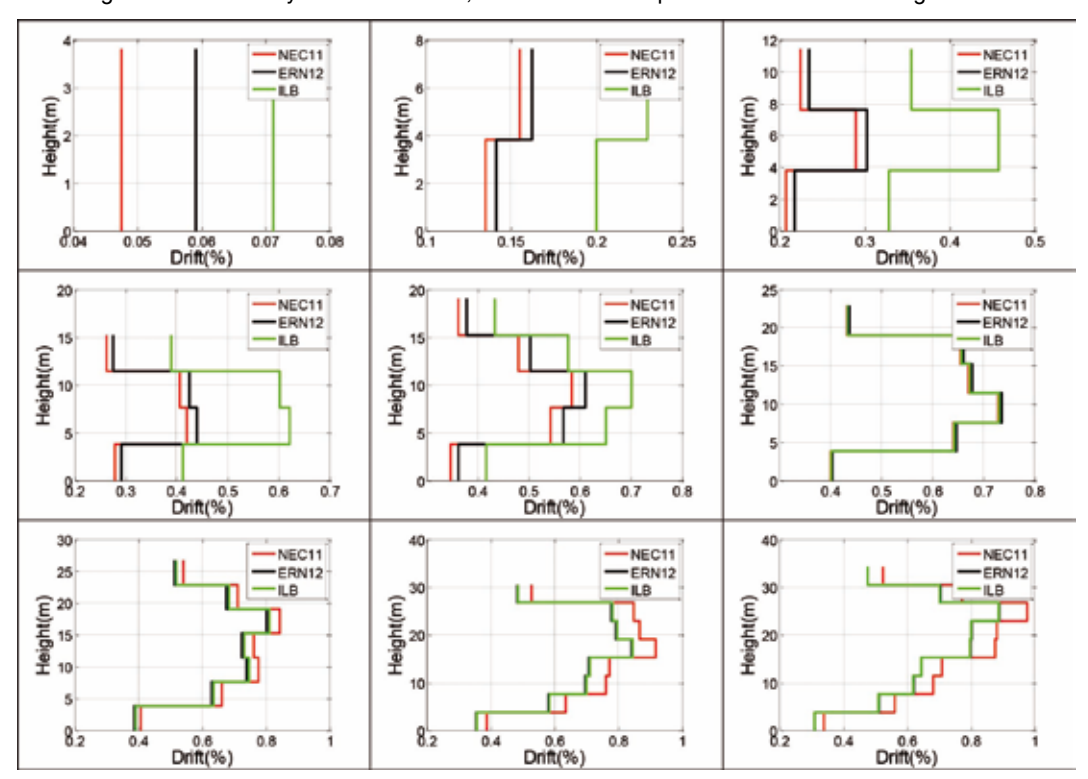


Table 6: Values of B with which the elastic spectrum is reduced, for the structures situated in the old Quito Tenis.

Floor	1	2	3	4	5	6	7	8	9
NEC	1	1	1	1	1	1.04	1.18	1.29	1.41
ERN	1	1	1	1	1	1	1	1	1
ILB	1	1	1	1	1	1.01	1.01	1.02	1.06

9 Comments and conclusions

The periods of recurrence that are expected in each of the segments of the blind inverse faults of Quito have been presented, for different ranges of magnitude, employing Gutenberg and Richter's model, modified and truncated. Subsequently, the microzoning found in North Central Quito is presented in the face of a probable earthquake of 6.2 magnitude, in the fault of Ilumbisí-La Bota.

For North Central Quito there are three spectra and they are those of the Ecuadorian Construction Regulations (Norma Ecuatoriana de la Construcción NEC-11); that found in the study of seismic microzoning, ERN-12 and that obtained from an earthquake in the fault Ilumbisi-La Bota which has been referred to as ILB. The big question is to find out with which spectrum, of the three, a structure should be designed. To answer the question, a seismic analysis was carried out of nine steel structures of 1 to 9 storeys, using the Capacity Spectrum Method and assuming that they are on three different sites in North Central Quito. The performance points found were obtained with the Capacity Spectrum Method/MEC, as well as the lateral displacements and the interstorey drifts, for the 27 cases of the study.

In order not to make the presentation too long, the performance point found in the Capacity Spectrum Method/MEC for the structures situated in the old Quito Tenis was presented; the maximum lateral displacements found in the structures of La Gasca and the interstorey drifts found in the structures situated in Colegio Benalcazar were also presented. It is noted that the lateral displacements and the interstorey drifts were obtained from the performance point.

From the study carried out, it can be concluded that for structures with periods less than 0.5 seconds the spectrum ILB should be used. In the study, these structures have 1 to 5 storeys. For structures with periods more than 0.5 seconds it cannot be said categorically that the spectrum of NEC-11 should be used because there was a case in which the largest responses were found with the spectrum ERN-12.

Considering that programs are currently available that facilitate seismic analysis, it is recommended that any structures that are going to be projected in North Central Quito be analyzed with the three spectra: NEC-11, ERN-12, and ILB.

10 References

Abrahamson N., Silva W., Kamai R. (2013), Update of the AS08 Ground-Motion Prediction Equations Based on the NGA-West2 Data Set. Pacific Earthquake Engineering Research Center, PEER, 143 p.

Abrahamson N., Silva W., Kamai R., (2014), "Summary of the ASK14 ground motion relation for active cristal regions", Earthquake Spectra, 30 (3), 1025-1055.

Aguiar Roberto, (2013), Microzonificación sísmica de Quito, Centro de Investigaciones Científicas. Universidad de Fuerzas Armadas, ESPE, Primera Edición, 212 p.

Aguiar Roberto, (2010), "Peligrosidad sísmica del Ecuador y descripción de los puentes construidos sobre el estuario del río Esmeraldas con aisladores de base FPS', Revista Internacional de Ingeniería de Estructuras, 15 (1), 85-118.

Aguiar Roberto, Mora David, Morales Enrique, (2015), "Peligrosidad sísmica de Quito y el Método del Espectro de Capacidad con CEINCI-LAB", Revista Internacional de Ingeniería de Estructuras, 20 (1), 1-39.

Aguiar Roberto, (1998), Acciones para el diseño sísmico de estructuras, Centro Internacional de Métodos Numéricos, CIMNE. Monografías de Ingeniería Sísmica, IS-30, 122 p.

Alvarado A., Audin L., Nocquet M., Lagreulet S., Segovia M., Font Y., Lamarque G., Yepes H., Mothes P., Rolandone F., Jarrín P., and Quidelleur X., (2014), "Active tectonics in Quito, Ecuador, assessed by geomorpholigical studies, GPS data, and crustal seismicity", Tectonics, AGUPLICATIONS, 17 p., Article online.

Bozorgnia, Y., Abrahamson, N., Al Atick, L., Ancheta, T., Atkinson, G., Baker, J., Rezaeian. (2014). NGA-West2 Research Project. Pacific Earthquake Engineering Research Center, University of California, Berkeley, CA.

Beauval C., Yepes H., Bakun W., Egred J., Alvarado A., and Singaucho C., (2010), "Locations and magnitudes of historical earthquakes in the Sierra of Ecuador (1586-1996), Geophys. Journal International, 181, 1613-1633.

Campbell K., Bozorgnia Y., (2013), NGA-West2 Campbell-Bozorgnia ground motion model for the horizontal components of PGA, PGV and 5%-Damped elastic Pseudo-Acceleration response spectra for periods ranging fro 0.01 to 10 sec, Pacific Earthquake Engineering Research Center, PEER, 75 p.

Elwood, K. (2013). Performance of concrete buildings in the 22 February 2011 Christchurch earthquake and implications for Canadian codes. Canadian Journal of Civil Engineering 40, 759-776.

ERN-2012, Microzonificación sísmica del distrito metropolitano de Quito: Estudio de la amenaza sísmica a nivel local. Programa para la reducción de riesgos urbanos. Distrito Metropolitano de Quito.

Leonard M., (2010), "Earthquake fault scaling: Self consistent relating of rupture length width, average displacement, and moment release", Bulletin of the Seismological Society of America, 100 (SA), 1971-1988.

Kam, W.Y., Pampanin, S. (2011). The seismic performance of RC buildings in the 22 February 2011 Christchurch earthquake. Structural Concrete 12 (4), 223-233.

NEC-11 (2014) Norma Ecuatoriana de la Construcción, Ministerio de Desarrollo Urbano y Vivienda, MIDUVI.

Rivas A., Aguiar R., Benito M. B., Gaspar J., Parra H., (2014), Determinación del período de recurrencia y magnitud máxima para el control de las estructuras en el rango elástico ante un sismo asociado a las fallas inversas de Quito, Revista Internacional de Ingeniería de Estructuras, 19 (2), 201-217.

Trujillo Santiago (2014), Espectro de Control para el Centro Norte de Quito, Tesis de Grado para obtener título de Ing. Civil. Universidad de Fuerzas Armadas ESPE, 95 p. Quito.

Espectros de diseño para el centro norte de quito y análisis sísmico de estructuras de acero por el método del espectro de capacidad

RESUMEN

La ciudad de Quito se halla sobre fallas geológicas, que no tienen afloramiento superficial pero están en movimiento con una velocidad de 2 a 4 mm., por año. El último sismo fuerte, asociado a estas fallas inversas, se registró en 1587 y tuvo una magnitud de 6.4; de tal manera que ha transcurrido más de 400 años con lo que la acumulación de energía es muy grande y la probabilidad de ocurrencia de un sismo es muy alta por lo que en este artículo se presenta en primer lugar los períodos de recurrencia de estas fallas; luego una microzonificación del Centro Norte de la ciudad y los espectros de respuesta elásticos para 5% de amortiguamiento asociados al segmento de falla Ilumbisí-La Bota, ILB. Posteriormente se analizan 9 estructuras de acero de 1 a 9 pisos, que se suponen están situadas en 3 diferentes suelos del Centro Norte de Quito y son los siguientes barrios: antiguo Quito Tenis; La Gasca; El Colegio Benalcazar. Se halla la respuesta sísmica, empleando el Método del Espectro de Capacidad MEC, ante tres espectros y son el prescrito en la Norma Ecuatoriana de la Construcción NEC-11; el recomendado en el estudio de microzonificación sísmica de Quito ERN-12 y los hallados en la micro zonificación sísmica asociados a la falla ILB. Para las estructuras ubicadas en el antiguo Quito Tenis se presenta el punto de desempeño hallado en el MEC; para las que se hallan en La Gasca se indican los desplazamientos laterales máximos en cada piso y para las estructuras ubicadas en el Colegio Benalcazar se presenta las derivas máximas de piso. Se destaca que a partir del punto de desempeño se hallan los desplazamientos laterales y derivas de piso, de tal manera que las conclusiones que se hallan en este estudio sobre con que espectro se tienen las máximas respuestas se pueden inferir con cualquiera de los tres parámetros estructurales.

Comentarios y conclusiones

Se ha presentado los períodos de recurrencia, que se esperan en cada uno de los segmentos de las fallas ciegas inversas de Quito, para diferentes rangos de magnitud, empleando el modelo de Gutenberg y Richter modificado y truncado. Posteriormente se presenta la micro zonificación encontrada en el Centro Norte de Quito ante un probable sismo de magnitud 6.2, en la falla de Ilumbisí-La Bota.

Para el Centro Norte de Quito se tienen tres espectros y son el de la Norma Ecuatoriana de la Construcción NEC-11; el hallado en el estudio de micro zonificación sísmica ERN-12 y el obtenido a partir de un sismo en la falla Ilumbisi-La Bota que se ha denominado ILB. La gran interrogante que se tiene es saber con que espectro, de los tres, se debe diseñar una estructura. Para contestar esta pregunta se realizó el análisis sísmico de 9 estructuras de 1 a 9 pisos de acero, por el Método del Espectro de Capacidad suponiendo que están situadas en tres sitios diferentes del Centro Norte y se obtuvieron los

puntos de desempeño hallados con el MEC, los desplazamientos laterales y las derivas de piso, para los 27 casos de estudio.

Para no alargar la presentación de resultados se presentó el punto de desempeño hallado en el MEC para las estructuras situadas en el antiguo Quito Tenis; los desplazamientos laterales máximos encontrados en las estructuras ubicadas en La Gasca y las derivas de piso halladas en las estructuras situadas en el Colegio Benalcazar. Se destaca que a partir del punto de desempeño se obtienen los desplazamientos laterales y las derivas de piso.

Del estudio realizado se concluye que para estructuras con períodos menores a 0.5 seg., se debe utilizar el espectro ILB. En el estudio estas estructuras son de 1 a 5 pisos. Para estructuras con períodos mayores a 0.5 seg., no se puede decir en forma categórica que se debe utilizar el espectro del NEC-11 porque hubo un caso en que las mayores respuestas se hallaron con el espectro ERN-12.

Considerando que actualmente se disponen de programas, que facilitan el análisis sísmico, se recomienda que las estructuras que se van a proyectar en el Centro Norte de Quito sean analizadas con los tres espectros: NEC-11, ERN-12, ILB.